International Journal of Biological Macromolecules 184 (2021) 159–169

Contents lists available at ScienceDirect

International Journal of Biological Macromolecules

journal homepage: www.elsevier.com/locate/ijbiomac

Synthesis of magnetic nanoparticles functionalized with histidine and nickel to immobilize His-tagged enzymes using β-galactosidase as a model

Bruna Coelho de Andrade [a], Adriano Gennari [a], Gaby Renard [b], Brenda Da Rolt Nervis [c], Edilson Valmir Benvenutti [d], Tania Maria Haas Costa [d], Sabrina Nicolodi [c], Nádya Pesce da Silveira [c], Jocelei Maria Chies [e], Giandra Volpato [f], Claucia Fernanda Volken de Souza [a,*]

[a] Food Biotechnology Laboratory, Biotechnology Graduate Program, University of Vale do Taquari - Univates, Lajeado, RS, Brazil
[b] National Institute of Science and Technology in Tuberculosis, Research Center for Molecular and Functional Biology, Pontifical Catholic University of Rio Grande do Sul, Porto Alegre, RS, Brazil
[c] Institute of Physics, Federal University of Rio Grande do Sul, Porto Alegre, Brazil
[d] Institute of Chemistry, Federal University of Rio Grande do Sul, Porto Alegre, Brazil
[e] Quatro G Pesquisa & Desenvolvimento Ltd., Porto Alegre, RS, Brazil
[f] Biotechnology course, Federal Institute of Education, Science, and Technology of Rio Grande do Sul - IFRS, Porto Alegre Campus, Porto Alegre, RS, Brazil

ARTICLE INFO

Keywords:
β-galactosidase
Nickel
Histidine

ABSTRACT

The aim of this study was to synthesize iron magnetic nanoparticles functionalized with histidine and nickel (Fe_3O_4-His-Ni) to be used as support materials for oriented immobilization of His-tagged recombinant enzymes of high molecular weight, using β-galactosidase as a model. The texture, morphology, magnetism, thermal stability, pH and temperature reaction conditions, and the kinetic parameters of the biocatalyst obtained were assessed. In addition, the operational stability of the biocatalyst in the lactose hydrolysis of cheese whey and skim milk by batch processes was also assessed. The load of 600 $U_{enzyme}/g_{support}$ showed the highest recovered activity value (~50%). After the immobilization process, the recombinant β-galactosidase (HisGal) showed increased substrate affinity and greater thermal stability (~50×) compared to the free enzyme. The immobilized β-galactosidase was employed in batch processes for lactose hydrolysis of skim milk and cheese whey, resulting in hydrolysis rates higher than 50% after 15 cycles of reuse. The support used was obtained in the present study without modifying chemical agents. The support easily recovered from the reaction medium due to its magnetic characteristics. The iron nanoparticles functionalized with histidine and nickel were efficient in the oriented immobilization of the recombinant β-galactosidase, showing its potential application in other high-molecular-weight enzymes.

1. Introduction

Enzyme immobilization is one of the strategies to reduce the disadvantages of using enzymes in industrial processes, such as lack of operational stability, and hard recovery and reuse of biocatalysts [1–4]. Enzymes can be immobilized via oriented or specific immobilization through the incorporation of affinity tags that selectively bind to a ligand in a solid matrix and guide enzyme binding on the support [5,6]. When compared to random immobilization, the oriented immobilization process may result in higher enzymatic activity [7].

Among these tags for recombinant enzyme production, His-tag stands out [6,8,9]. The production of recombinant proteins tagged with His-tag at the N-terminal or C-terminal has been widely used to apply enzymes in industrial processes [10–12]. The main advantages of using this tag are the addition of few amino acids to the protein chain of the enzyme and easy incorporation into a target protein [13–16]. The interaction between the His-tag imidazole group and nickel enables targeted and reversible binding of the recombinant enzyme to an immobilization support material containing this metal [17–19]. The inclusion of tags can also help in the evaluation of

* Corresponding author at: Food Biotechnology Laboratory, Biotechnology Graduate Program, University of Vale do Taquari - Univates, Avenida Avelino Tallini, 171, 95914-014 Lajeado, RS, Brazil.
E-mail address: claucia@univates.br (C.F. Volken de Souza).

https://doi.org/10.1016/j.ijbiomac.2021.06.060
Received 2 March 2021; Received in revised form 31 May 2021; Accepted 9 June 2021
Available online 11 June 2021

biochemical characteristics of proteins through different in silico techniques [20–25].

Magnetic nanoparticles (MNPs) are suitable supports for enzyme immobilization because they have characteristics such as easy separation of the immobilized enzyme by means of a magnetic field, a high surface area that allows a high enzymatic load, a significant enzyme-substrate interaction, and the possibility of functionalizing their surface [1,26–29]. Studies have focused on developing MNPs to purify His-tagged proteins using single-stage processes [18,30–34].

The functionalization technique employed to purify or immobilize His-tagged enzymes is usually performed with nitrilotriacetic acid (NTA) or derivatives [15,31,35,36]. However, Rashid et al. [30] reported a simpler method to synthesize MNPs, by adding only histidine-Ni, not using NTA. Rashid et al. [30] used this synthesized material to interact with Protein-A histidines containing His-tag, a protein of low molecular weight (42 kDa), to easily purify this recombinant protein.

The β-galactosidase enzyme is used to process milk and dairy products, resulting in low-lactose or lactose-free products and food supplements for individuals with lactose intolerance [37–39]. β-galactosidases are also able to produce galacto-oligosaccharides (GOS), which are prebiotic functional ingredients used as substrates to grow beneficial intestinal microbiota [40,41].

To the best of our knowledge, no studies have investigated the production of His-tagged β-galactosidase linked to MNPs of Fe_3O_4 modified with histidine and nickel (Fe_3O_4-His-Ni) for application in lactose hydrolysis. Due to the growing number of intolerants to this disaccharide, this study aimed to synthesize nanoparticles of Fe_3O_4-His-Ni to serve as support to oriented immobilization of recombinant His-tagged enzymes of high molecular weight, using β-galactosidase as a model. The texture, morphology, magnetism, thermal stability, pH and temperature reaction conditions, and kinetic parameters of the biocatalyst obtained were assessed. In addition, the operational stability of the biocatalyst in the lactose hydrolysis of cheese whey and skim milk by batch processes was assessed.

2. Materials and methods

2.1. Materials

The genomic DNA from *Kluyveromyces* sp. was extracted using the Wizard Genomic DNA Purification kit (Promega®, Brazil). Restriction enzymes (*Nde*I *e Xho*I) were acquired from Biolabs® (São Paulo, Brazil), the pCR-Blunt cloning vector from Invitrogen® (California, US), and *Pfu* Turbo DNA polymerase from Quatro G P&D (Rio Grande do Sul, Brazil). The plasmid DNA extraction kit (QIAprep Spin Miniprep Kit) was purchased from QIAGEN® (Hilden, Germany), and the expression vector pET-30a(+) from Novagen® (Merck, Germany). The Ortho-nitrophenyl-β-D-galactopyranoside (ONPG) was purchased from Sigma-Aldrich® (St. Louis, USA). The glucose quantification kit was acquired from Labtest® (Minas Gerais, Brazil), and the culture media from Merck® (Darmstadt, Germany). Skim milk was purchased from Brazil Foods S.A. (Rio Grande do Sul, Brazil), and cheese whey was provided by Arla Foods (Córdoba, Argentina). The other substances used were analytical-grade reagents (Sigma-Aldrich®, Missouri, US), and culture media, provided by Merck® (Darmstadt, Germany).

2.2. Methods

2.2.1. Preparation of magnetic nanoparticles modified with histidine and nickel

Histidine magnetic nanoparticles (MNP-His) were synthesized using the chemical co-precipitation method [30,42]. Iron salts (4.20 g of $FeCl_3.6H_2O$ and 2.16 g of $FeCl_2.4H_2O$) were dissolved in 100 mL of ultrapure water in a nitrogen atmosphere. The mixture was heated at 90 °C under constant magnetic stirring (Velp Scientifica®, RS, Brazil), and 3.10 g of L-histidine and 30 mL of 30% (v/v) NH_4OH were added to the solution. The suspension remained under stirring at 90 °C for 6 h. Nanoparticles were collected by centrifugation (Hettich®, Universal 320R, Germany) (2370 ×*g*, at 4 °C, for 5 min), washed four times with ultrapure water, and vacuum-dried (Solab®, SL104/27, Brazil) at 60 °C and −10 mmHg to obtain MNP-His.

To bind nickel to MNP-His, 0.5 g of MNP-His were kept in an ultrasonic bath (Unique®, USC1450, Brazil) (25 kHz, 60 min) in 100 mL of ethanol, forming a homogeneous dispersion. Ethanol was removed by centrifugation (Hettich®, Universal 320R, Germany) (2370 ×*g*, at 4 °C, for 5 min), then 100 mL of 0.5 M $NiCl_2$ were added. The solution was kept in an orbital shaking incubator (Marconi®, MA830, Brazil) at 25 °C, 150 rpm, overnight. The nickel-modified MNP-His (MNP-His-Ni) were separated using a magnet, washed with ethanol four times to remove the non-reagent $NiCl_2$, and vacuum-dried at 60 °C and −10 mmHg [31].

2.2.2. Amplification and cloning of the β-galactosidase enzyme encoding gene

The genomic DNA was extracted from *Kluyveromyces* sp. in a previous study [43]. The β-galactosidase (Gal) gene of *Kluyveromyces* sp. (GenBank: M84410.1) was amplified by a polymerase chain reaction (PCR) in a thermal cycler programmed at 95 °C for 2.0 min, 30 cycles of 95 °C for 30 s, 60 °C for 30 s, 72 °C for 3.0 min, and a final elongation of 72 °C for 10 min, using *Pfu* turbo DNA polymerase enzyme and specific oligonucleotide primers (*forward primer* 5′ –GCCATATGCATCATCATCATCATCATTCTTGCCTTATTCCTGAG – 3′ and *reverse primer* 5′ – CCTTAAGTCCCTCGAGTTATTCAAAAGCGAGATCAAAC – 3′) with binding sites for *Nde*I and *Xho*I (underlined) restriction enzymes and with a polyhistidine tag (6×-His) in 2.5% of dimethyl sulfoxide (DMSO). The amplified DNA fragment was cloned into a pCR-Blunt vector and subcloned into a pET-30a (+) expression vector. The *Escherichia coli* DH10B strain was transformed by electroporation (2.45 kV, 200 Ω, 25 μF) (BioRad®, Gene Pulser II, US) with pET-30a(+):HisGal construction. The entire gene length of the recombinant β-galactosidase carrying an N-terminal His-tag was sequenced using specific primers (Table S1, Supplementary material). The sequences were analyzed using the Basic Local Alignment Search Tool (BLAST®) program.

2.2.3. Expression of recombinant β-galactosidase

The pre-inoculum was obtained from an isolated *E. coli* BL21(DE3) strain transformed with pET-30a(+): HisGal was kept overnight in a Luria-Bertani (LB) medium (10 g/L NaCl, 10 g/L tryptone, 5 g/L yeast extract), in the presence of kanamycin (50 μg/mL), at 37 °C and 180 rpm in an orbital shaking incubator (Marconi®, MA830, Brazil). The transformed *E. coli* cells were grown in 250-mL Erlenmeyer flasks, containing 50 mL of LB culture medium and the specific antibiotic. The initial optical density (OD_{600nm}) was standardized at 0.1, measured in a spectrophotometer (Shimadzu®, UV-2600, Japan). Cultures were kept at 37 °C and 180 rpm in an orbital shaking incubator. When the OD_{600nm} reached values ranging from 0.4 to 0.6, the expression of HisGal was induced by adding 10 g/L of lactose to the cultures. The expression occurred at 30 °C, under a 180-rpm stirring speed, for 24 h. Cells were centrifuged at 4 °C, 11,000 ×*g*, for 10 min (Hitachi®, CR 22G III, Japan). For cell disruption, 5 g of cells were resuspended in 50 mL of lysis buffer (pH 7.5, 100 mM NaH_2PO_4, 500 mM NaCl, 20 mM imidazole, 1 mM *Phenylmethylsulfonyl fluoride* (PMSF)) and disrupted in a *French* press (Constant Systems Ltd.®, Cell Disruption Systems, United Kingdom) (30 kpsi). The soluble and insoluble fractions were separated by centrifugation (Hitachi®, CR 21G, Japan) (at 4 °C, 38900 ×*g*, for 30 min).

2.2.4. Immobilization of β-galactosidase enzyme

HisGal immobilization was performed by mixing 50 mg MNP-His-Ni and 10 mL of soluble fraction diluted in Buffer A (100 mM NaH_2PO_4, 500 mM NaCl, and 20 mM imidazole, pH 7.5) for the enzymatic loads of 600, 1200, 1800, and 2400 $U_{enzyme}/g_{support}$. Immobilization was conducted in a roller mixer (Didática®, MR II, Brazil) at 25 °C and 150 rpm

for 30 min. As a control, the enzymatic solutions were incubated under the same conditions in the absence of MNP-His-Ni. During the immobilization process, periodic collections were carried out to determine the parameters of immobilization, yield, efficiency, and recovered activity, as shown in Eqs. (1), (2), and (3), respectively [44].

$$Yield\ (\%) = \frac{Initial\ activity - Supernatant\ activity}{Initial\ activity} \times 100 \quad (1)$$

$$Efficiency\ (\%) = \frac{Derivative\ activity}{Initial\ activity - Supernatant\ activity} \times 100 \quad (2)$$

$$Recovered\ activity\ (\%) = \frac{Derivative\ activity}{Initial\ activity} \times 100 \quad (3)$$

Immobilized HisGal in MNP-His-Ni was separated using a magnet. The derivative (MNP-His-Ni-HisGal) (Fig. 1) was washed three times with Buffer A and kept in the same buffer under refrigeration (4 °C) for future assessment. The immobilization time effect (10, 30, 45, and 60 min) was assessed for the best load reached.

All experiments were carried out in triplicate. Statistical verification of the immobilization parameters (yield, efficiency, and recovered activity) was performed through a one-way analysis of variance (ANOVA). Fisher's F-test determined the significance of the model. In the significant models, the Tukey Test was performed with a significance level of 0.05 (p-value <0.05) to compare the means. BioEstat 5.0 was used in the statistical analysis of the results.

2.2.5. Free and immobilized β-galactosidase activity

Free enzyme (HisGal) and immobilized enzyme (MNP-His-Ni-HisGal) activity was determined using the ortho-Nitrophenyl-β-galactoside (ONPG) chromogenic substrate, following the methodology proposed by Rech et al. with some modifications [45]. In the analysis, 100 μL of free enzyme or derivative were added to 1000 μL of substrate solution (13 mM ONPG in 50 mM of potassium phosphate buffer, pH 7.0, containing 3 mM of $MgCl_2$). The reaction was carried out at 30 °C, and after 1 min, 200 μL of Na_2CO_3 1 M were added. For the immobilized enzyme, the reaction was carried out for 2 min under constant stirring. The absorbance reading was performed on a spectrophotometer (Shimadzu®, UV-2600, Japan) at a 405-nm wavelength. One unit of activity (U) was defined as the amount of enzyme that catalyzes the release of 1 μmol of ortho-nitrophenol (ONP) per minute under assay conditions.

2.2.6. Characterization of nanoparticles and immobilized β-galactosidase: Morphology, structure, magnetism, and texture

The MNP-His, MNP-His-Ni, and MNP-His-Ni-HisGal samples were observed using the Field-Emission Scanning Electron Microscope (FESEM) (FEI®, Inspect F50, Japan) with an acceleration voltage of 20 kV and a magnification of 150,000× for the structural morphology analysis. The samples were dispersed in isopropanol, added to carbon ribbon, then metalized with gold, and observed in FESEM. The elemental composition of the samples was determined by Energy Dispersive Spectroscopy (EDS) (FEI®, Inspect F50, Japan), with an acceleration voltage of 20 kV.

The zeta potential of the MNP-His, MNP-His-Ni, and MNP-His-Ni-HisGal samples was determined using ZetaPlus (Brookhaven Instruments, USA) at 25 °C. The samples were resuspended at a 1:5 ratio in a Buffer A solution.

The infrared spectra of the MNP-His, MNP-His-Ni, and MNP-His-Ni-HisGal samples were obtained using the Shimadzu FTIR Instrument (Prestige 21, Japan). The KBr technique was used to obtain spectra with a 4-cm^{-1} resolution and 100 cumulative scans.

The thermogravimetric analysis (TGA) of the MNP-His, MNP-His-Ni, and MNP-His-Ni-HisGal samples was performed using a Shimadzu Thermal Analyzer (TA50, Japan) at a 20 °C/min heating rate, under room temperature up to 900 °C under an argon atmosphere. The samples were previously degassed at 60 °C under vacuum for 18 h.

The magnetic properties of the MNP-His, MNP-His-Ni, and MNP-His-Ni-HisGal samples were assessed using a vibrating sample magnetometer (VSM) (MicroSense®, EZ9, USA). The samples magnetization curves ($M \times H$) were obtained through field sweeping between −20 and +20 kOe at room temperature.

Textural characterization of the MNP-His, MNP-His-Ni, and MNP-His-Ni-HisGal samples was performed using N_2 adsorption-desorption isotherms at liquid N_2 boiling temperature using a Micromeritics device (Tristar Kr 3020, USA). The samples were previously degassed at 60 °C under vacuum for 18 h. The Brunauer–Emmett–Teller (BET) multipoint technique determined the specific surface area, and the pore size distribution was obtained through Density Functional Theory (DFT) [46].

2.2.7. Characterization of the catalytic properties of free and immobilized β-galactosidase

The tests of optimal pH and temperature of the free (HisGal) and immobilized (MNP-His-Ni-HisGal) enzymes were performed based on the enzymatic activity at pH values ranging between 5.5 and 8.0 (at 30 °C) and temperatures between 20 and 70 °C (pH 7.0) for 2 min at 150 rpm. In each test (pH or temperature), the highest activity value obtained was 100%, and it was used to calculate the relative enzymatic activity.

The kinetic parameters of the free and immobilized enzymes were determined using different ONPG concentrations (6.5 to 52 mM) for 2 min at 150 rpm and 30 °C. The K_M (Michaelis constant) values and V_{max} (maximum rate of reaction) were determined employing the Michaelis-Menten model and the Lineweaver-Burk linearization, following Eq. (4).

$$\frac{1}{V} = \frac{KM}{Vmax} \times \frac{1}{[S]} + \frac{1}{Vmax} \quad (4)$$

where V (mM·min^{-1}) is the catalytic reaction rate, V_{max} (mM·min^{-1}) is maximum speed, [S] is substrate concentration (mM), and K_M is the Michaelis-Menten constant (mM).

To determine the thermal stability of free and immobilized enzymes, samples were incubated in a water bath (Marconi®, MA 156, Brazil) at 45, 48, 50, and 53 °C. The residual enzymatic activity was determined at different incubation periods. Thermodynamic parameters were calculated following the deactivation model described in the literature [47].

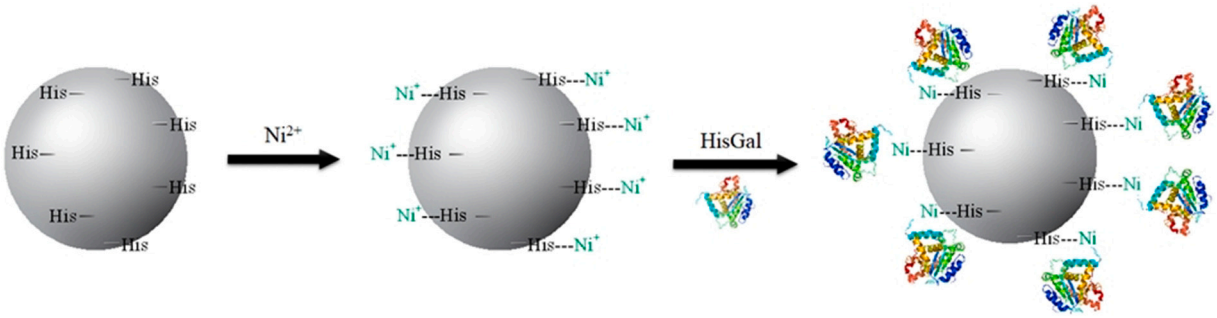

Fig. 1. Schematic representation of the HisGal immobilization process in MNP-His-Ni.

The activation energy (E_a) for inactivation was calculated through non-linear regression, following the Arrhenius graph (Eq. (5)).

$$k = A.e^{-\frac{Ea}{RT}} \quad (5)$$

where k (min^{-1}) is the deactivation kinetic constant, A (min^{-1}) is the pre-exponential factor, E_a ($J{\cdot}mol^{-1}$) is the activation energy, R (8,314 $J{\cdot}mol^{-1}{\cdot}K^{-1}$) is the universal gas constant, and T (K) is temperature.

The half-life time ($t_{1/2}$) of an enzyme is the time needed for the initial activity to decrease to half of its value (Eq. (6)).

$$t1/2 = ln\ 2/k \quad (6)$$

The stabilization factor (SF) at each temperature was calculated by dividing the half-life time of the immobilized enzyme by the half-life time of the free enzyme.

Gibbs free energy for thermal inactivation (ΔG) was calculated based on the inactivation constant at different temperatures (Eq. (7)):

$$\Delta G = -R.T.ln\left(\frac{k.h}{k_B.T}\right) \quad (7)$$

where R (8.314 $J{\cdot}mol^{-1}{\cdot}K^{-1}$) is the universal gas constant, T (K) is temperature, k (min^{-1}) is the deactivation kinetic constant, h (6.6262×10^{-34} J·s) is the Planck constant, and k_B (1.3806×10^{-23} $J{\cdot}K^{-1}$) is the Boltzmann constant.

The enthalpy change (ΔH) was calculated using the activation energy ($\Delta H = E_a - RT$), and the entropy change (ΔS) using enthalpy changes and Gibbs free energy ($T\Delta S = \Delta H - \Delta G$). All characterization experiments were carried out in triplicate and shown as mean ± standard deviation.

2.2.8. Assessment of the reusability of immobilized β-galactosidase

The reuse of immobilized β-galactosidase in MNP-His-Ni samples was assessed through lactose hydrolysis tests in batch processes using cheese whey and skim milk, both reconstituted to 5% (w/v) lactose. Tests were carried out with 100 mg of MNP-His-Ni-HisGal (600 U/g of β-galactosidase) in 5 mL of cheese whey and skim milk solutions in a roller mixer (Didática®, MRII, Brazil) at 25 °C, 150 rpm for 30 min. By the end of each enzyme reuse cycle, the immobilized enzyme was recovered by centrifugation (1000 ×*g*, 1 min, 25 °C) and the supernatant fluid was collected to establish the degree of hydrolysis using the colorimetric enzyme kit of oxidase-peroxidase (Labtest®, Glucose Liquiform, Brazil) to form glucose. The derivative was washed with 5 mL of Buffer A. A new solution of cheese whey or skim milk was added, starting a new cycle of reuse of MNP-His-Ni-HisGal. The degree of hydrolysis of the derivative after the first reuse cycle was defined as 100% hydrolysis. The recycled nanoparticles were characterized in relation to morphology, structure, magnetism, and texture, according to the methodologies described in Section 2.2.6.

3. Results and discussion

3.1. Expression and immobilization of the recombinant β-galactosidase enzyme

The gene of interest was cloned and expressed in *E. coli* BL21 (DE3). The sequencing of the *Kluyveromyces* sp. β-galactosidase gene indicated that the recombinant protein's primary structure is composed of 1032 amino acids. The recombinant DNA alignment presented an identity of 99%, respectively, with the β-galactosidase gene of *Kluyveromyces marxianus* and *Kluyveromyces lactis*. Expression of the recombinant enzyme (120 kDa) in the soluble and insoluble fractions, was verified.

Table 1 shows different loads of HisGal immobilized in MNP-His-Ni in 30 min. Considering the immobilization yield, the enzymatic loads of 1200, 1800, and 2400 $U_{enzyme}/g_{support}$ showed the highest results. However, the highest rate of immobilization efficiency was obtained using the load of 600 $U_{enzyme}/g_{support}$. Our results showed that the MNP-His-Ni support allows good yield for immobilization. Nonetheless, loads higher than 600 $U_{enzyme}/g_{support}$ may result in support overload. The excess of immobilized enzymes may have led to a steric impediment of the active site of β-galactosidase or to conformational changes in enzyme molecules immobilized in the support [48,49]. Variations in immobilization efficiency with loadings higher than 600 U/g may have been caused by the interaction of β-galactosidase with other proteins that were present in the enzyme extract, thus having a positive or negative effect on the activity of the model enzyme. Since the recovered activity takes into account the efficiency results, recovered activity also varied. Thus, the enzymatic load of 600 $U_{enzyme}/g_{support}$ was chosen to assess the effects of the other immobilization times (10, 45, and 60 min) since it presented the highest values of immobilization efficiency and recovered activity.

Table 1
Effect of different loads on the immobilization parameters of β-galactosidase (HisGal) on magnetic nanoparticles modified with histidine and nickel (MNP-His-Ni).

Enzymatic load ($U_{enzyme}/g_{support}$)	Yield (%)	Efficiency (%)	Recovered activity (%)
600	65.86 ± 8.24[b]	75.27 ± 3.80[a]	49.42 ± 3.70[a]
1200	83.05 ± 0.39[a]	32.09 ± 2.40[c]	26.72 ± 1.99[c]
1800	84.38 ± 2.02[a]	46.10 ± 6.14[b]	38.82 ± 6.41[b]
2400	78.96 ± 6.55[a]	25.23 ± 2.88[c]	18.41 ± 2.66[c]

Different letters in the same column represent a significant difference ($p < 0.05$). Each value represents the mean of three experiments conducted in duplicate and the standard deviation.

Carli et al. [35] used a methodology similar to ours by synthesizing cross-linked Fe_3O_4 nanoparticles with chitosan/glutaraldehyde/N-(5-amino-1-carboxy-pentyl) iminodiacetic acid functionalized with $NiCl_2$ [35]. They immobilized endonuclease (Egst) and β-glucosidase (Bglhi) proteins, both containing a histidine tag. Carli et al. [35] immobilized 3 U of Egst and 1 U of Bglhi and obtained an efficiency of 132% and 115% and yields of 21% and 20%, respectively. In the present study, a higher enzymatic load of HisGal was immobilized in MNP-His-Ni, with yield values of about 80%. Khan et al. [49] applied β-galactosidase in the immobilization process using magnetic graphene oxide nanocomposites (Gr@Fe_3O_4NCS) and observed that increased concentrations of immobilized enzymes (from 1 mg/mL to the 2–5 mg/mL range) reduced the process yield [49]. This behavior can be attributed to the theory of diffusion limitation [49], which was also observed in the present study.

At the other periods of immobilization (10, 45, and 60 min), efficiency and recovered activity results were below those obtained for 30 min, 75% and 49%, respectively. Therefore, the characterization assays of the immobilized enzyme were carried out with a load of 600 $U_{enzyme}/g_{support}$ and 30 min of immobilization time.

3.2. Characterization of nanoparticles and immobilized β-galactosidase: morphology, structure, magnetism, and texture

The morphological characteristics of MNP-His, MNP-His-Ni, and MNP-His-Ni-HisGal were visualized using FESEM, as shown in Fig. 2. The morphology of MNPs did not change after the immobilization process, keeping their spherical shape. MNP-His, MNP-His-Ni, and MNP-His-Ni-HisGal showed mean diameters of 41.03 ± 4.07 nm, 39.21 ± 4.17 nm, and 40.92 ± 3.95 nm, respectively, and formed agglomerated structures due to the natural attraction of nanoparticles caused by magnetism. Magnetic particles produced by Rashid et al. [30] showed an almost spherical shape and average diameter of 30–35 nm [30]. These sizes are similar to those obtained in the present study, as the particles were non-coated in both works. In Gennari et al. [50], the magnetic particles coated

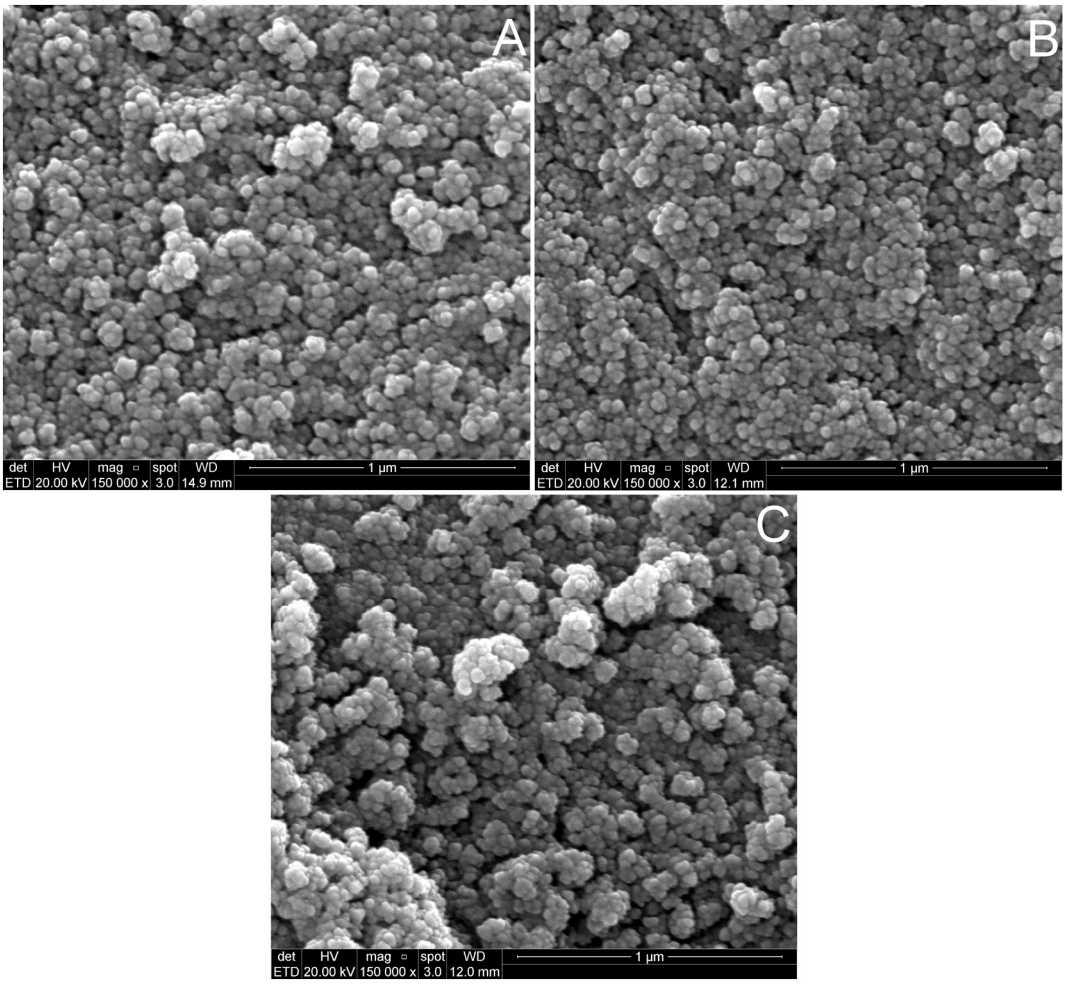

Fig. 2. Field-Emission Scanning Electron Microscope (FESEM) images of the samples: (A) MNP-His, (B) MNP-His-Ni, and (C) MNP-His-Ni-HisGal samples.

with nanocellulose showed an average diameter approximately 2 times larger (74 nm) when compared to these non-coated particles [50].

The elemental composition of MNPs showed 67% iron in MNP-His-Ni, 72% iron and 2.38% nickel in MNP-His-Ni, and 55% iron in MNP-His-Ni-HisGal. Our equipment did not detect nickel in the derivative. The immobilization of the recombinant enzyme reduced the proportion of iron, which is attributed to the incorporation of carbon and oxygen of protein structures.

The zeta potential of the MNP-His, MNP-His-Ni, and MNP-His-Ni-HisGal samples was 8.16, −7.63, and −38.78 mV, respectively. These values show the stability of these systems and that the particles of the derivative formed a more stable system than that of others, for having a higher modulus value. Liou et al. [51] also reported an increase in system stability after immobilization when studying the production of cross-linked polypeptide/enzyme microgels using the catalase enzyme (CAT) and *star*-shaped poly(L-lysine) (PLL) [51]. Since zeta potential indicates the stability of a colloidal system, magnetic particles that have a high zeta potential value (negative or positive) repel and form a stable system [52], which is a desirable characteristic when applying immobilized enzymes [53].

Fig. 3 shows the infrared spectra of MNP-His, MNP-His-Ni, and MNP-His-Ni-HisGal. A strong band, with a maximum size of about 580 cm^{-1}, was attributed to Fe—O stretching of magnetite particles [54]. The band of 1635 cm^{-1} is related to the C—O stretching of the carboxyl group [30]. However, water bending cannot be discarded for the MNP-His-Ni and MNP-His-Ni-HisGal spectra since these samples also present a broad band above 3000 cm^{-1} due to O—H stretching of adsorbed water [30]. A new broad band appeared after enzyme immobilization, with maximum value of about 1100 cm^{-1}. As reported by Gennari et al. [55], this band was attributed to the chemical groups of β-galactosidase [55].

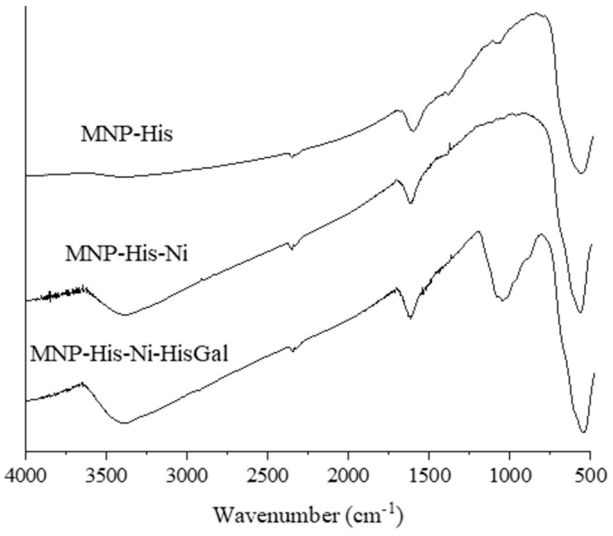

Fig. 3. Infrared spectra of MNP-His, MNP-His-Ni, and MNP-His-Ni-HisGal.

Table 2
Mass variation (%) of MNP-His, MNP-His-Ni, and MNP-His-Ni-HisGal at different temperature ranges.

Sample	Temperature range (°C)				
	25–150	150–400	400–500	500–700	700–900
MNP-His	−1.79	−4.21	−0.34	−0.30	−0.25
MNP-His-Ni	−2.01	−1.68	−0.41	−0.83	−0.39
MNP-His-Ni-HisGal	−4.08	−2.33	−0.19	−0.50	−1.12

We assessed the thermal stability of MNP-His, MNP-His-Ni, and MNP-His-Ni-HisGal using TGA (Table 2). The results show a low loss of mass (5% to 9%) in the three samples for the range of temperature assessed. At the first stage (25 to 150 °C), the decrease in mass in the three materials was attributed to the evaporation of adsorbed water [56]. The second stage of loss of mass (above 200 °C) may be explained by the degradation of histidine imidazole rings present in magnetite nanoparticles [57]. At this temperature range, the MNP-His sample suffered a sudden loss of mass. Suo et al. [58] found similar results of loss of mass at temperatures above 250 °C [58]. Comparing the three samples, greater heat stability was observed for MNP-His-Ni, followed by MNP-His-Ni-HisGal, which showed lower losses of mass between 150 and 400 °C (Table 2). The greatest loss of mass of MNP-His-Ni-HisGal, 2.33% (from 150 to 400 °C), may indicate the beginning of degradation of immobilized β-galactosidase. The MNP-His sample showed an increase in mass between 400 and 500 °C due to the oxidation reaction of magnetite to hematite with the incorporation of oxygen to the oxide [59]. However, for the MNP-His-Ni and MNP-His-Ni-HisGal samples, small losses of mass were observed in this temperature range between 400 and 500 °C, probably due to the partial decomposition in the argon atmosphere of the organic matter in the samples stabilized with Ni in the range between 150 and 400 °C, which formed a protective layer around the magnetite and prevented or delayed its oxidation [60]. In the temperature range of 500 to 700 °C, the MNP-His-Ni and MNP-His-Ni-HisGal samples showed greater losses of mass than the MNP-His sample. These losses were related to the carbonization of the samples [61]. Long et al. [62] observed this behavior in the temperature range of 200 to 600 °C, which was attributed to the organic decomposition of the immobilized enzymes [62]. In our study, considering the temperature range from 150 to 900 °C, the NPM-His-Ni-HisGal sample showed a mass loss rate 0.83% higher than that of the NPM-His-Ni sample, probably because of the enzyme incorporated in the system.

We assessed the effects of changes in MNPs and immobilization on the magnetic hysteresis properties of materials (Fig. 4).

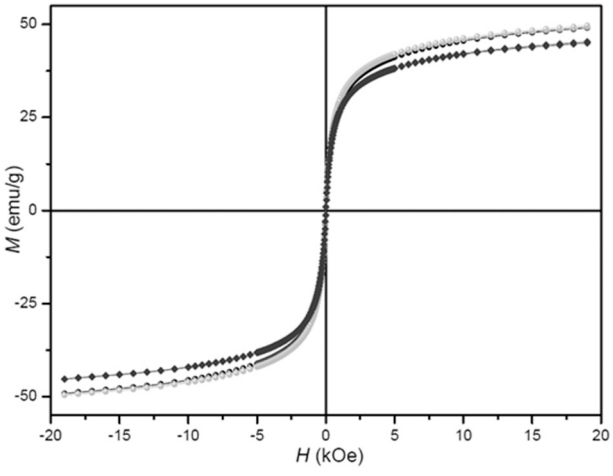

Fig. 4. Magnetization curves of modified magnetic nanoparticles (MNP-His and MNP-His-Ni) and the derivative obtained (MNP-His-Ni-HisGal). (●) MNP-His, (●) MNP-His-Ni, (◆) MNP-His-Ni-HisGal.

We determined the magnetic properties of the MNP-His, MNP-His-Ni, and MNP-His-Ni-HisGal samples to assess the effect of the immobilization process. Findings showed a typical response of a predominantly superparamagnetic system, presenting relatively low $M_r/M(H_{max})$ coercivity and remission and no saturation for relatively intense fields (~20 kOe) at room temperature. According to these criteria, the nanoparticles obtained were classified as soft due to their narrow hysteresis cycles. The saturation magnetization obtained in the maximum available field $M(H_{max})$ was affected, while the coercive field showed no difference between treatments. The $M(H_{max})$ values of the nanoparticles (MNP-His) remained mostly stable (~49 emu/g) before and after nickel modification (MNP-His-Ni). After the immobilization of β-galactosidase (MNP-His-Ni-HisGal), $M(H_{max})$ decreased to about 45 emu/g. According to Bezerra et al. [63], the saturation magnetization value is expected to decrease due to the increase in the amount of mass bound to the material [63].

Hosseini et al. [64] synthesized MNPs of Fe_3O_4 (MN), modified the material with chitosan (CMN), and then immobilized it with the lipase enzyme (LCMN) of *Candida antarctica* [64]. Regarding magnetic characteristics, the saturation magnetization values were 78 (MN), 36 (CMN), and 31 (LCMN) emu/g. Hosseini et al. [64] identified a marked decrease in saturation magnetization in particles coated with chitosan and in the material after immobilization when compared to MN [64]. This drop in saturation magnetization results from the addition of mass to MN, including chitosan, which is a high-molecular-weight polymer, and the enzyme used by the authors. We also observed a decrease in saturation magnetization after immobilizing the recombinant β-galactosidase (49 to 45 emu/g). However, nickel modification did not produce a similar behavior, probably due to the low amount of mass added to the magnetic material.

Table 3 and Fig. 5 show the textural characteristics of modified MNPs (MNP-His and MNP-His-Ni) and the derivative obtained (MNP-His-Ni-HisGal).

Fig. 5a presents the adsorption-desorption isotherms, and Fig. 5b and c show the DFT pore size distribution curves. The MNP-His and MNP-His-Ni materials presented similar characteristics in the microporosity region, i.e. in low relative P/P_0 pressures. The micropores (diameter < 2.0 nm) contributed to the surface area, and there were no significant changes after nickel addition. However, changes in high relative P/P_0 pressures were found in isotherms after nickel addition. The high-pressure region is related to the mesopores that contributed to the pore volume. After enzyme immobilization (MNP-His-Ni-HisGal), a marked decrease was observed in the surface area. This effect was interpreted as a consequence of the decrease in microporosity, which is evident in isotherms and in the DFT micropore size distribution. This feature may be a consequence of the enzymes covering the surface, which blocked the access of micropores. Enzyme immobilization did not cause significant changes in the mesopore characteristics, as illustrated in the isotherms and pore size distribution curves.

Gennari et al. [50] synthesized a magnetic material by binding nanocrystalline cellulose to MNPs [50]. The authors used this material as support to the immobilization of β-galactosidase enzymes of *Aspergillus oryzae* and *Kluyveromyces lactis* microorganisms. Assessing textural characteristics, Gennari et al. [50] observed a decrease in the surface area (up to 50%) and volume of the pores (up to 60%) of the support used for both enzymes after immobilization. Matte et al. [65] studied the

Table 3
Textural properties of modified magnetic nanoparticles (MNP-His and MNP-His-Ni) and the derivative obtained (MNP-His-Ni-HisGal).

Sample	BET surface area (m^2/g)	BJH pore volume (cm^3/g)
MNP-His	109 ± 4	0.389 ± 0.001
MNP-His-Ni	116 ± 4	0.280 ± 0.001
MNP-His-Ni-HisGal	83 ± 3	0.263 ± 0.001

Results expressed as mean ± standard deviation.

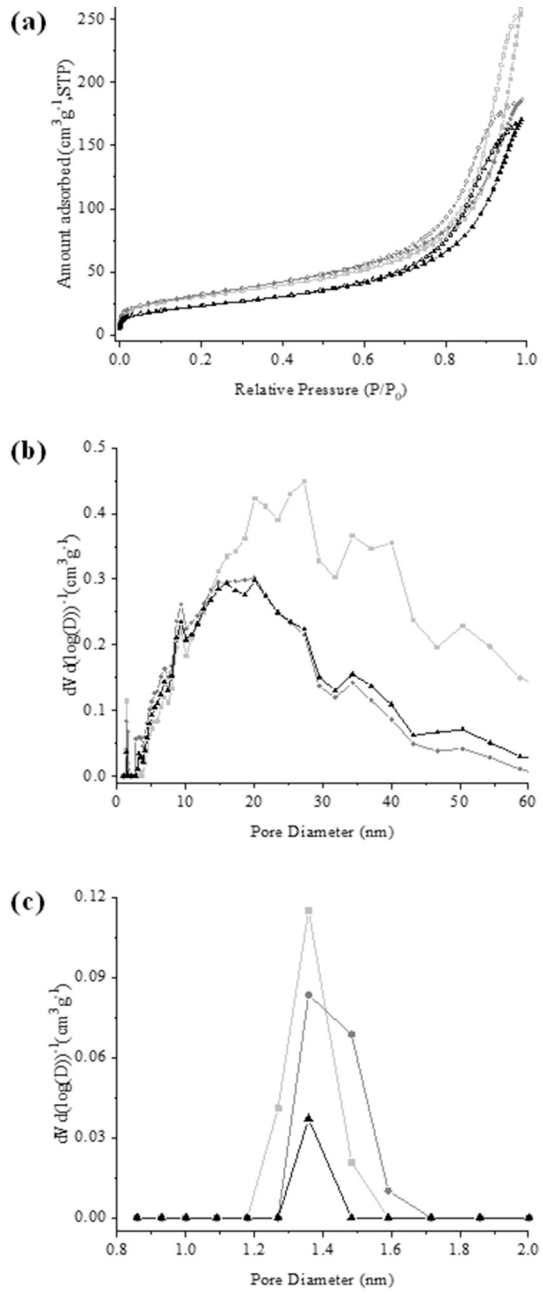

Fig. 5. Textural analysis of magnetic nanoparticles before and after immobilization. (a) Isotherms of nitrogen adsorption (■, ●, ▲) and desorption (□, ○, △) and characteristics of (b) micro and (c) mesopores. (■) MNP-His, (●) MNP-His-Ni, (▲) MNP-His-Ni-HisGal.

physicochemical properties of the Immobead 150 support before and after lipase immobilization [65]. The immobilization process resulted in a decrease in the specific surface area and volume of the pores from 137 to 63 m^2/g, and 0.37 cm^3/g to 0.25 cm^3/g, respectively. According to Matte et al. [65], this decrease in values resulted from enzyme molecule coating of the support surface.

3.3. Characterization of the catalytic properties of free and immobilized β-galactosidase

Fig. 6a shows the effect of different pH values on HisGal and MNP-His-Ni-HisGal activities. The immobilization of recombinant β-galactosidase did not change the optimal pH (6.0) in the hydrolysis reaction.

The optimal pH was similar for both enzymes, with relative activity above 80% in the pH range of 6.0 to 6.5. Gennari et al. [50] found similar results in their study, in which the commercial *Kluyveromyces lactis* β-galactosidase was immobilized in magnetic nanocellulose particles [50]. The immobilized enzyme was less susceptible to operational changes, and the optimal pH did not change due to the immobilization process.

Fig. 6b shows the effect of temperature on HisGal and MNP-His-Ni-HisGal activities. The immobilization of recombinant β-galactosidase did not affect the optimum temperature (60 °C) in the hydrolysis catalysis.

Both enzymes showed low activity at low temperatures and reached more than 50% of relative activity above 40 °C. When compared to the free β-galactosidase (HisGal), the immobilized β-galactosidase (MNP-His-Ni-HisGal) showed higher values of relative activity at 70 and 75 °C. Khan et al. [49] observed similar behavior for β-galactosidase immobilized on Gr@Fe_3O_4NCS: both enzymes showed the same optimum temperature (50 °C), and the immobilized enzyme showed higher relative activity (71%) than the free β-galactosidase (31%) at 70 °C [49]. Gracida et al. [66] and Mohamad et al. [67] claimed that the immobilization process can provide higher enzymatic stability and resistance against enzymatic denaturation because of temperature [66,67].

Table 4 shows the kinetic parameters of HisGal and MNP-His-Ni-HisGal. The K_M value evidenced that the affinity of recombinant β-galactosidase with the substrate increased after immobilization, indicating that the process favored the binding energy between the active enzyme site and the substrate (ONPG). This result may be due to the oriented immobilization of HisGal in the MNP-His-Ni support. However, the V_{max} value decreased after immobilization, possibly due to a greater difficulty of diffusion of the immobilized enzyme and/or changes in the microenvironment around the biocatalyst [68].

Park et al. [69] immobilized the β-glucosidase enzyme in modified MNPs with (3-aminopropyl) triethoxysilane (APTES)/glutaraldehyde [69]. Regarding the kinetic parameters, Park et al. [69] also reported a decrease in V_{max} values after the immobilization process due to the diffusion limitations of the substrate and the factors that might have altered the three-dimensional structure of the immobilized enzyme [69]. Gracida et al. [66] immobilized the xylanase enzyme on Fe_3O_4 particles containing chitosan and also observed a decrease in the K_M value in relation to the free enzyme, showing that immobilization enabled a strong affinity between the enzyme (E) and the substrate (S) by stabilizing the transition state $E_{immobilized}$-S [66].

We determined the thermal stability of MNP-His-Ni-HisGal and HisGal using thermal and thermodynamic parameters, as seen in Table 5. The immobilized enzyme was more thermally stable than the free enzyme at all temperatures assessed. The values obtained for the deactivation kinetic constant (k), the half-life time ($t_{1/2}$), and the stabilization factor (SF) evidenced this result. This thermal resistance was stronger at the highest temperature assessed (53 °C), in which MNP-His-Ni-HisGal showed k and $t_{1/2}$ values 53× lower and 67× higher, respectively, than the values obtained for HisGal. The ΔG value increased, while the ΔS value decreased after β-galactosidase immobilization. This indicates that MNP-His-Ni-HisGal was more resistant to denaturation and that the immobilized enzyme was less prone to conformational changes, consequently presenting higher thermal stability [70]. These results showed the importance of immobilization to improve the thermal stability of enzymes, as already reported by other authors [1,71–73].

3.4. Assessment of reusability of immobilized β-galactosidase

The immobilized β-galactosidase (MNP-His-Ni-HisGal) was applied in batch processes for lactose hydrolysis. After 15 cycles of reuse, the immobilized enzyme hydrolyzed 60% and 40% of disaccharide of skim milk and cheese whey, respectively (Fig. 6c). The decrease in hydrolysis throughout the reuse cycles may be explained by enzymatic inactivation and loss of mass of the immobilized enzyme due to the washes

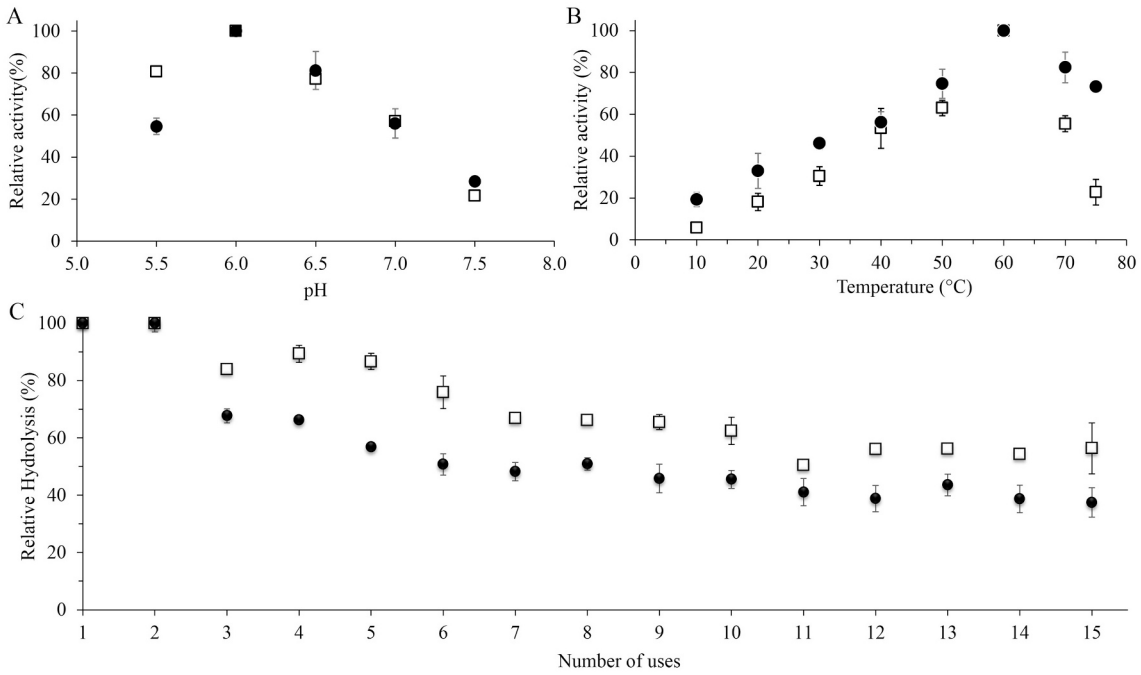

Fig. 6. (A) Effect of different pH values and (B) temperatures on the activity of free β-galactosidase (HisGal) (□) and immobilized β-galactosidase (MNP-His-Ni-HisGal) (●); (C) Reusability of immobilized β-galactosidase (MNP-His-Ni-HisGal) for lactose hydrolysis in (□) skim milk and (●) cheese way, both reconstituted with 5% (w/v) lactose.

Table 4
Kinetic parameters of β-galactosidase (HisGal) and immobilized β-galactosidase (MNP-His-Ni-HisGal).

Enzyme	K_M (mM)	V_{max} (mM/min)
HisGal	5.40 ± 0.50	3.58 ± 0.14
MNP-His-Ni-HisGal	1.50 ± 0.26	1.06 ± 0.26

Results expressed as mean ± standard deviation.

Table 5
Thermodynamic parameters and thermal inactivation parameters for free (HisGal) and immobilized (MNP-His-Ni-HisGal) β-galactosidase.

		Enzyme	
		HisGal	MNP-His-Ni-HisGal
45 °C	k (min^{-1})	0.48 ± 0.10	0.15 ± 0.01
	$t_{1/2}$ (min)	1.48 ± 0.29	4.77 ± 0.10
	SF	–	3.27 ± 0.60
	ΔH ($kJ{\cdot}mol^{-1}$)	9.75 ± 0.96	2.28 ± 0.09
	ΔG ($kJ{\cdot}mol^{-1}$)	91.41 ± 1.04	93.98 ± 0.05
	ΔS ($J{\cdot}mol^{-1}{\cdot}K^{-1}$)	−256.77 ± 0.27	−288.35 ± 0.27
48 °C	k (min^{-1})	3.87 ± 0.04	0.69 ± 0.10
	$t_{1/2}$ (min)	0.18 ± 0.01	1.16 ± 0.19
	SF	–	5.82 ± 0.85
	ΔH ($kJ{\cdot}mol^{-1}$)	9.73 ± 0.96	2.26 ± 0.09
	ΔG ($kJ{\cdot}mol^{-1}$)	86.13 ± 0.03	90.78 ± 0.62
	ΔS ($J{\cdot}mol^{-1}{\cdot}K^{-1}$)	−238.01 ± 2.90	−275.78 ± 1.64
50 °C	k (min^{-1})	14.02 ± 0.15	1.03 ± 0.06
	$t_{1/2}$ (min)	0.05 ± 0.00	0.71 ± 0.08
	SF	–	14.23 ± 0.56
	ΔH ($kJ{\cdot}mol^{-1}$)	9.71 ± 0.96	2.24 ± 0.09
	ΔG ($kJ{\cdot}mol^{-1}$)	83.22 ± 0.56	90.35 ± 0.30
	ΔS ($J{\cdot}mol^{-1}{\cdot}K^{-1}$)	−227.59 ± 2.96	−272.79 ± 0.64
53 °C	k (min^{-1})	55.26 ± 0.25	1.04 ± 0.03
	$t_{1/2}$ (min)	0.01 ± 0.00	0.67 ± 0.02
	SF	–	53.28 ± 1.44
	ΔH ($kJ{\cdot}mol^{-1}$)	9.69 ± 0.96	2.22 ± 0.09
	ΔG ($kJ{\cdot}mol^{-1}$)	80.31 ± 0.69	91.08 ± 0.07
	ΔS ($J{\cdot}mol^{-1}{\cdot}K^{-1}$)	−216.62 ± 2.94	−272.59 ± 0.45

SF = Stabilization Factor.
Results expressed as mean ± standard deviation.

carried out after each cycle [71,74,75]. The recycled nanoparticles showed an approximate increase of 10% in their surface area, and their morphology, structure, and magnetism did not change after the reuse cycles. The variation in the degree of hydrolysis between the dairy products assessed may be related to the optimum pH of the immobilized enzyme and to cheese whey composition, which contains proteins and minerals that may inhibit β-galactosidase. Verma et al. [76] immobilized *Kluyveromyces lactis* β-galactosidase in silicon dioxide nanoparticles functionalized with glutaraldehyde. They observed that the immobilized enzyme kept approximately 50% of its ONPG hydrolysis activity after 11 cycles of reuse [76]. In the reuse cycles with cheese whey and skim milk as substrates, the immobilized enzyme (MNP-His-Ni-HisGal) showed easy recovery from the reaction medium due to the magnetic characteristics of the support, enabling the industrial application of the enzyme.

Huang et al. [77] and Verma et al. [78] also evaluated the use of magnetic nanoparticle-based supports for the immobilization of high-molecular-weight proteins. Huang et al. [77] immobilized the enzyme β-glucosidase (100 kDa) on magnetic manganese dioxide nanoparticles (Fe_3O_4@MnO_2). The immobilized enzyme showed increased thermal stability and maintained activity of over 60% after 8 cycles in the reuse process [77]. Similarly, Verma et al. [78] immobilized the enzyme β-glucosidase on iron oxide magnetic nanoparticles and found the same behavior reported in our study. The immobilized enzyme showed higher thermal stability compared to the free enzyme and maintained approximately half of the enzyme activity after 16 reuse cycles [78]. In the present study, we achieved a similar stability by employing a recombinant His-tagged enzyme for immobilization on the support developed.

4. Conclusion

This study reported the development of MNPs modified with histidine and nickel for oriented immobilization of high-molecular-

weight proteins containing His-tag, using β-galactosidase as a model. We immobilized an enzymatic load of 600 $U_{enzyme}/g_{support}$, with yield and efficiency rates higher than 84 and 75%, respectively. The kinetic parameters changed after immobilization since the enzyme's affinity with the substrate increased, as indicated by the decrease in K_M. At the highest temperature (53 °C), the thermal stability of the immobilized enzyme was approximately 50× higher than that of free β-galactosidase. The immobilized enzyme was applied 15 times in batch processes in lactose hydrolysis in skim milk and cheese whey, reaching hydrolysis rates higher than 50%. This study presents a support synthesized through a simple process without modification with chemical agents. This support was easily separated from the reaction medium and allowed oriented immobilization of high-molecular-weight proteins with histidine tail. The present study aims to continue this investigation using other metals, such as cobalt and zinc, for the functionalization of MNPs, aiming at the immobilization of high-molecular-weight proteins.

Supplementary data to this article can be found online at https://doi.org/10.1016/j.ijbiomac.2021.06.060.

CRediT authorship contribution statement

- Bruna Coelho de Andrade: Conceptualization, Investigation, Methodology, Formal Analysis, Writing-Original Draft Preparation, and Writing-Reviewing and Editing.
- Adriano Gennari: Conceptualization, Investigation, Methodology, Formal Analysis, Writing-Original Draft Preparation, and Writing-Reviewing and Editing.
- Gaby Renard: Conceptualization, Methodology, Formal Analysis, Writing-Original Draft Preparation, and Writing-Reviewing and Editing.
- Brenda Da Rolt Nervis: Investigation, and Methodology.
- Edilson Valmir Benvenutti: Methodology, Formal Analysis, and Writing-Original Draft Preparation.
- Tania Maria Haas Costa: Methodology, Formal Analysis, and Writing-Original Draft Preparation.
- Sabrina Nicolodi: Methodology, Formal Analysis, and Writing-Original Draft Preparation.
- Nádya Pesce da Silveira: Formal Analysis, and Writing-Original Draft Preparation.
- Jocelei Maria Chies: Resources, and Supervision.
- Giandra Volpato: Conceptualization, Formal Analysis, Resources, Supervision, Writing-Original Draft Preparation, and Writing-Reviewing and Editing.
- Claucia Fernanda Volken de Souza: Conceptualization, Investigation, Methodology, Formal Analysis, Resources, Supervision, Writing-Original Draft Preparation, and Writing-Reviewing and Editing.

Declaration of competing interest

The authors declare they do not have any conflicts of interest.

Acknowledgments

We would like to thank the Brazilian Council for Scientific and Technological Development (CNPq) (grant no. 311655/2017-3, 315225/2018-1, and 420506/2016-0), Brazilian Coordination for the Improvement of Higher Education Personnel (CAPES), and Foundation for Research of the state of Rio Grande do Sul (FAPERGS) for the scholarships granted, and the University of Vale do Taquari - Univates for the financial support granted for this research paper. We would also like to thank the company Quatro G Pesquisa & Desenvolvimento Ltd. for their support in the experiment. This study was partially funded by CAPES – Finance Code 001.

References

[1] V.D. Nguyen, G. Styevkó, E. Madaras, G. Haktanirlar, A.T.M. Tran, E. Bujna, M. S. Dam, Q.D. Nguyen, Immobilization of ß-galactosidase on chitosan-coated magnetic nanoparticles and its application for synthesis of lactulose-based galactooligosaccharides, Process Biochem. 84 (2019) 30–38, https://doi.org/10.1016/j.procbio.2019.05.021.
[2] Neelam, A.K. Chhillar, J.S. Rana, Enzyme nanoparticles and their biosensing applications: a review, Anal. Biochem. 581 (2019), 113345, https://doi.org/10.1016/j.ab.2019.113345.
[3] A.A. Homaei, R. Sariri, F. Vianello, R. Stevanato, Enzyme immobilization: an update, J. Chem. Biol. 6 (2013) 185–205, https://doi.org/10.1007/s12154-013-0102-9.
[4] W. Huang, S. Pan, Y. Li, L. Yu, R. Liu, Immobilization and characterization of cellulase on hydroxy and aldehyde functionalized magnetic Fe2O3/Fe3O4 nanocomposites prepared via a novel rapid combustion process, Int. J. Biol. Macromol. 162 (2020) 845–852, https://doi.org/10.1016/j.ijbiomac.2020.06.209.
[5] K. Hernandez, R. Fernandez-Lafuente, Control of protein immobilization: coupling immobilization and site-directed mutagenesis to improve biocatalyst or biosensor performance, Enzym. Microb. Technol. 48 (2011) 107–122, https://doi.org/10.1016/j.enzmictec.2010.10.003.
[6] D.A. Butterfield, D. Bhattacharyya, S. Daunert, L. Bachas, Catalytic biofunctional membranes containing site-specifically immobilized enzyme arrays: a review, J. Memb. Sci. 181 (2001) 29–37, https://doi.org/10.1016/S0376-7388(00)00342-2.
[7] J.R. Simons, M. Mosisch, A.E. Torda, L. Hilterhaus, Site directed immobilization of glucose-6-phosphate dehydrogenase via thiol-disulfide interchange: influence on catalytic activity of cysteines introduced at different positions, J. Biotechnol. 167 (2013) 1–7, https://doi.org/10.1016/j.jbiotec.2013.06.002.
[8] C.C. Yu, Y.Y. Kuo, C.F. Liang, W.T. Chien, H.T. Wu, T.C. Chang, F.D. Jan, C.C. Lin, Site-specific immobilization of enzymes on magnetic nanoparticles and their use in organic synthesis, Bioconjug. Chem. 23 (2012) 714–724, https://doi.org/10.1021/bc200396r.
[9] B. Koo, N.S. Dolan, K. Wucherer, H.K. Munch, M.B. Francis, Site-selective protein immobilization on polymeric supports through N-terminal imidazolidinone formation, Biomacromolecules 20 (2019) 3933–3939, https://doi.org/10.1021/acs.biomac.9b01002.
[10] M. Bilal, H.M.N. Iqbal, S. Guo, H. Hu, W. Wang, X. Zhang, State-of-the-art protein engineering approaches using biological macromolecules: a review from immobilization to implementation view point, Int. J. Biol. Macromol. 108 (2018) 893–901, https://doi.org/10.1016/j.ijbiomac.2017.10.182.
[11] M. Bilal, H.M.N. Iqbal, Tailoring multipurpose biocatalysts via protein engineering approaches: a review, Catal. Letters. 149 (2019) 2204–2217, https://doi.org/10.1007/s10562-019-02821-8.
[12] J. Döbber, M. Pohl, HaloTagTM: evaluation of a covalent one-step immobilization for biocatalysis, J. Biotechnol. 241 (2017) 170–174, https://doi.org/10.1016/j.jbiotec.2016.12.004.
[13] X. Li, S. Song, Y. Pei, H. Dong, T. Aastrup, Z. Pei, Oriented and reversible immobilization of His-tagged proteins on two- and three-dimensional surfaces for study of protein-protein interactions by a QCM biosensor, Sensors Actuators B Chem. 224 (2016) 814–822, https://doi.org/10.1016/j.snb.2015.10.096.
[14] X. Zhao, G. Li, S. Liang, Several affinity tags commonly used in chromatographic purification, J. Anal. Methods Chem. 2013 (2013), https://doi.org/10.1155/2013/581093.
[15] A.M. Shemsi, F.A. Khanday, A. Qurashi, A. Khalil, G. Guerriero, K.S. Siddiqui, Site-directed chemically-modified magnetic enzymes: fabrication, improvements, biotechnological applications and future prospects, Biotechnol. Adv. 37 (2019) 357–381, https://doi.org/10.1016/j.biotechadv.2019.02.002.
[16] M.B. Méndez, C.W. Rivero, F. López-Gallego, J.M. Guisán, J.A. Trelles, Development of a high efficient biocatalyst by oriented covalent immobilization of a novel recombinant 2'-N-deoxyribosyltransferase from Lactobacillus animalis, J. Biotechnol. 270 (2018) 39–43, https://doi.org/10.1016/j.jbiotec.2018.01.011.
[17] K. Terpe, Overview of tag protein fusions: from molecular and biochemical fundamentals to commercial systems, Appl. Microbiol. Biotechnol. 60 (2003) 523–533, https://doi.org/10.1007/s00253-002-1158-6.
[18] G. Cao, J. Gao, L. Zhou, Z. Huang, Y. He, M. Zhu, Y. Jiang, Fabrication of Ni2 -nitrilotriacetic acid functionalized magnetic mesoporous silica nanoflowers for one pot purification and immobilization of His-tagged O-transaminase, Biochem. Eng. J. 128 (2017) 116–125, https://doi.org/10.1016/j.bej.2017.09.019.
[19] J.P. Lata, L. Gao, C. Mukai, R. Cohen, J.L. Nelson, L. Anguish, S. Coonrod, A. J. Travis, Effects of nanoparticle size on multilayer formation and kinetics of tethered enzymes, Bioconjug. Chem. 26 (2015) 1931–1938, https://doi.org/10.1021/acs.bioconjchem.5b00354.
[20] B.C. de Andrade, L.F.S.M. Timmers, G. Renard, G. Volpato, C.F.V. de Souza, Microbial β-Galactosidases of industrial importance: computational studies on the effects of point mutations on the lactose hydrolysis reaction, Biotechnol. Prog. 36 (2020) 1–9, https://doi.org/10.1002/btpr.2982.
[21] R. Singh, V.K. Bhardwaj, J. Sharma, P. Das, R. Purohit, Discovery and in silico evaluation of aminoarylbenzosuberene molecules as novel checkpoint kinase 1 inhibitor determinants, Genomics 113 (2021) 707–715, https://doi.org/10.1016/j.ygeno.2020.10.001.
[22] R. Singh, V. Bhardwaj, P. Das, R. Purohit, Natural analogues inhibiting selective cyclin-dependent kinase protein isoforms: a computational perspective, J. Biomol. Struct. Dyn. 38 (2020) 5126–5135, https://doi.org/10.1080/07391102.2019.1696709.

[23] V.K. Bhardwaj, R. Purohit, Targeting the protein-protein interface pocket of Aurora-A-TPX2 complex: rational drug design and validation, J. Biomol. Struct. Dyn. (2020) 1–10, https://doi.org/10.1080/07391102.2020.1772109.
[24] G. Tanwar, R. Purohit, Gain of native conformation of Aurora a S155R mutant by small molecules, J. Cell. Biochem. 120 (2019) 11104–11114, https://doi.org/10.1002/jcb.28387.
[25] C. Gopalakrishnan, B. Kamaraj, R. Purohit, Mutations in microRNA binding sites of CEP genes involved in cancer, Cell Biochem. Biophys. 70 (2014) 1933–1942, https://doi.org/10.1007/s12013-014-0153-8.
[26] M. Abbaszadeh, P. Hejazi, Metal affinity immobilization of cellulase on Fe3O4 nanoparticles with copper as ligand for biocatalytic applications, Food Chem. 290 (2019) 47–55, https://doi.org/10.1016/j.foodchem.2019.03.117.
[27] O. Kvitek, A. Reznickova, A. Zelenakova, V. Zelenak, M. Orendac, V. Svorcik, Immobilization of Fe@Au superparamagnetic nanoparticles on polyethylene, Eur. Polym. J. 110 (2019) 56–62, https://doi.org/10.1016/j.eurpolymj.2018.10.043.
[28] P.A. Johnson, H.J. Park, A.J. Driscoll, Enzyme nanoparticle fabrication: magnetic nanoparticle synthesis and enzyme immobilization, Methods Mol. Biol. (2010) 183–191, https://doi.org/10.1007/978-1-60761-895-9.
[29] J. Fauser, S. Savitskiy, M. Fottner, V. Trauschke, B. Gulen, Sortase-mediated quantifiable enzyme immobilization on magnetic nanoparticles, Bioconjug. Chem. 31 (2020) 1883–1892, https://doi.org/10.1021/acs.bioconjchem.0c00322.
[30] Z. Rashid, H. Naeimi, A.H. Zarnani, F. Mohammadi, R. Ghahremanzadeh, Facile fabrication of nickel immobilized on magnetic nanoparticles as an efficient affinity adsorbent for purification of his-tagged protein, Mater. Sci. Eng. C. 80 (2017) 670–676, https://doi.org/10.1016/j.msec.2017.07.014.
[31] L.A.B.C. Carneiro, R.J. Ward, Functionalization of paramagnetic nanoparticles for protein immobilization and purification, Anal. Biochem. 540–541 (2018) 45–51, https://doi.org/10.1016/j.ab.2017.11.005.
[32] H. Guo, H. Sun, Z. Su, S. Hu, X. Wang, Fe3O4@PAM@NTA-Ni2 magnetic composite nanoparticles for highly specific separation of His-tagged proteins, J. Wuhan Univ. Technol. Mater. Sci. Ed. 33 (2018) 559–565, https://doi.org/10.1007/s11595-018-1860-6.
[33] L. Jose, C. Lee, A. Hwang, J.H. Park, J.K. Song, H. Paik, Magnetically steerable Fe3O4 @Ni2 -NTA-polystyrene nanoparticles for the immobilization and separation of his6-protein, Eur. Polym. J. 112 (2019) 524–529, https://doi.org/10.1016/j.eurpolymj.2019.01.024.
[34] M. Shin, B. Kang, N. Yoon, Synthesis of Fe3O4@nickel–silicate core–shell nanoparticles for His-tagged enzyme immobilizing agents, Nanotechnology 27 (2016) 1–9, https://doi.org/10.1088/0957-4484/27/49/495705.
[35] S. Carli, L.A.B.C. Carneiro, R.J. Ward, L.P. Meleiro, Immobilization of a ß-glucosidase and an endoglucanase in ferromagnetic nanoparticles: a study of synergistic effects, Protein Expr. Purif. 160 (2019) 28–35, https://doi.org/10.1016/j.pep.2019.03.016.
[36] Y. Zhang, Y. Yang, W. Ma, J. Guo, Y. Lin, C. Wang, Uniform magnetic core/shell microspheres functionalized with Ni2 -iminodiacetic acid for one step purification and immobilization of His-ragged enzymes, ACS Appl. Mater. Interfaces 5 (2013) 2626–2633, https://doi.org/10.1021/am4006786.
[37] S.A. Ansari, Q. Husain, Lactose hydrolysis by ß-galactosidase immobilized on concanavalin A-cellulose in batch and continuous mode, J. Mol. Catal. B Enzym. 63 (2010) 68–74, https://doi.org/10.1016/j.molcatb.2009.12.010.
[38] S. Erich, B. Kuschel, T. Schwarz, J. Ewert, N. Böhmer, F. Niehaus, J. Eck, S. Lutz-Wahl, T. Stressler, L. Fischer, Novel high-performance metagenome ß-galactosidases for lactose hydrolysis in the dairy industry, J. Biotechnol. 210 (2015) 27–37, https://doi.org/10.1016/j.jbiotec.2015.06.411.
[39] Á. Pereira-Rodríguez, R. Fernández-Leiro, M.I. González-Siso, M.E. Cerdán, M. Becerra, J. Sanz-Aparicio, Structural basis of specificity in tetrameric Kluyveromyces lactis ß-galactosidase, J. Struct. Biol. J. 177 (2012) 392–401, https://doi.org/10.1016/j.jsb.2011.11.031.
[40] Y.N. Dong, H.Q. Chen, Y.H. Sun, H. Zhang, W. Chen, A differentially conserved residue (Ile42) of GH42 ß-galactosidase from Geobacillus stearothermophilus BgaB is involved in both catalysis and thermostability, J. Dairy Sci. 98 (2015) 2268–2276, https://doi.org/10.3168/jds.2014-9117.
[41] D.O. Otieno, Synthesis of ß-galactooligosaccharides from lactose using microbial ß-galactosidases, Compr. Rev. Food Sci. Food Saf. 9 (2010) 471–482, https://doi.org/10.1111/j.1541-4337.2010.00121.x.
[42] H.M. Jiang, Z.P. Yan, Y. Zhao, X. Hu, H.Z. Lian, Zincon-immobilized silica-coated magnetic Fe3O4 nanoparticles for solid-phase extraction and determination of trace lead in natural and drinking waters by graphite furnace atomic absorption spectrometry, Talanta 94 (2012) 251–256, https://doi.org/10.1016/j.talanta.2012.03.035.
[43] B.C. de Andrade, V.F. Migliavacca, F.Y. Okano, V.Y. Grafulin, J. Lunardi, G. Roth, C.F.V. de Souza, D.S. Santos, J.M. Chies, G. Volpato, Production of recombinant ß -galactosidase in bioreactors by fed-batch culture using DO-stat and linear control, Biocatal. Biotransform. 37 (2019) 3–9, https://doi.org/10.1080/10242422.2018.1493105.
[44] R.A. Sheldon, S. van Pelt, Enzyme immobilisation in biocatalysis: why, what and how, Chem. Soc. Rev. 42 (2013) 6223–6235, https://doi.org/10.1039/C3CS60075K.
[45] R. Rech, C. Cassini, A. Secchi, M. Ayub, Utilization of protein-hydrolyzed cheese whey for production of ß-galactosidase by Kluyveromyces marxianus, J. Ind. Microbiol. Biotechnol. 23 (1999) 91–96, https://doi.org/10.1038/sj.jim.2900692.
[46] P. Webb, C. Orr, R. Camp, J. Olivier, Y. Yunes, Analytical methods in fine particle technology, in: Micromeritics Instrument, first ed., 1997.
[47] B.A. Kikani, S.P. Singh, Enzyme stability, thermodynamics and secondary structures of a-amylase as probed by the CD spectroscopy, Int. J. Biol. Macromol. 81 (2015) 450–460, https://doi.org/10.1016/j.ijbiomac.2015.08.032.
[48] J. Han, L. Wang, Y. Wang, J. Dong, X. Tang, L. Ni, L. Wang, Preparation and characterization of Fe3O4-NH2@4-arm-PEG-NH2, a novel magnetic four-arm polymer-nanoparticle composite for cellulase immobilization, Biochem. Eng. J. 130 (2018) 90–98, https://doi.org/10.1016/j.bej.2017.11.008.
[49] M. Khan, Q. Husain, A.H. Naqvi, Graphene based magnetic nanocomposites as versatile carriers for high yield immobilization and stabilization of ß-galactosidase, RSC Adv. 6 (2016) 53493–53503, https://doi.org/10.1039/c6ra06960f.
[50] A. Gennari, F.H. Mobayed, B.R. Nervis, E.V. Benvenutti, S. Nicolodi, N.P. da Silveira, G. Volpato, C.F.V. de Souza, Immobilization of ß-galactosidases on magnetic nanocellulose: textural morphological, magnetic, and catalytic properties, Biomacromolecules 20 (2019) 2315–2326, https://doi.org/10.1021/acs.biomac.9b00285.
[51] J.H. Liou, Z.H. Wang, I.H. Chen, S.S. Wang, S.C. How, J.S. Jan, Catalase immobilized in polypeptide/silica nanocomposites via emulsion and biomineralization with improved activities, Int. J. Biol. Macromol. 159 (2020) 931–940, https://doi.org/10.1016/j.ijbiomac.2020.05.138.
[52] B. Sahoo, S.K. Sahu, P. Pramanik, A novel method for the immobilization of urease on phosphonate grafted iron oxide nanoparticle, J. Mol. Catal. B Enzym. 69 (2011) 95–102, https://doi.org/10.1016/j.molcatb.2011.01.001.
[53] X. Qiu, S. Wang, S. Miao, H. Suo, H. Xu, Y. Hu, Co-immobilization of laccase and ABTS onto amino-functionalized ionic liquid-modified magnetic chitosan nanoparticles for pollutants removal, J. Hazard. Mater. 401 (2021), 123353, https://doi.org/10.1016/j.jhazmat.2020.123353.
[54] Q.Y. Huang, M. Hiyama, T. Kabe, S. Kimura, T. Iwata, Enzymatic self-biodegradation of poly(l-lactic acid) films by embedded heat-treated and immobilized proteinase K, Biomacromolecules 21 (2020) 3301–3307, https://doi.org/10.1021/acs.biomac.0c00759.
[55] A. Gennari, F.H. Mobayed, R.S. Rafael, A.L. Catto, E.V. Benvenutti, R.C. Rodrigues, R.A. Sperotto, G. Volpato, C.F.V. de Souza, Stabilization study of tetrameric Kluyveromyces lactis ß-galactosidase by immobilization on immobead: thermal, physico-chemical, textural and catalytic properties, Braz. J. Chem. Eng. 36 (2019) 1403–1417, https://doi.org/10.1590/0104-6632.20190364s20190235.
[56] J.K. Poppe, A.P.O. Costa, M.C. Brasil, R.C. Rodrigues, M.A.Z. Ayub, Multipoint covalent immobilization of lipases on aldehyde-activated support: characterization and application in transesterification reaction, J. Mol. Catal. B Enzym. 94 (2013) 57–62, https://doi.org/10.1016/j.molcatb.2013.05.017.
[57] X. Wan, X. Xiang, S. Tang, D. Yu, H. Huang, Y. Hu, Immobilization of Candida antarctic lipase B on MWNTs modified by ionic liquids with different functional groups, Colloids Surf. B Biointerfaces. 160 (2017) 416–422, https://doi.org/10.1016/j.colsurfb.2017.09.037.
[58] H. Suo, L. Xu, Y. Xue, X. Qiu, H. Huang, Y. Hu, Ionic liquids-modified cellulose coated magnetic nanoparticles for enzyme immobilization: improvement of catalytic performance, Carbohydr. Polym. 234 (2020), 115914, https://doi.org/10.1016/j.carbpol.2020.115914.
[59] R.M. Ashour, R. El-sayed, A.F. Abdel-Magied, A.A. Abdel-khalek, M.M. Ali, K. Forsberg, A. Uheida, M. Muhammed, J. Dutta, Selective separation of rare earth ions from aqueous solution using functionalized magnetite nanoparticles: kinetic and thermodynamic studies, Chem. Eng. J. 327 (2017) 286–296, https://doi.org/10.1016/j.cej.2017.06.101.
[60] A. Vedaei-Sabegh, J.B. Morin, M. Jahazi, Influence of nickel on high-temperature oxidation and characteristics of oxide layers in two high-strength steels, Steel Res. Int. 91 (2020) 1–13, https://doi.org/10.1002/srin.201900536.
[61] K.S. Muthuvelu, R. Rajarathinam, R.N. Selvaraj, V.B. Rajendren, A novel method for improving laccase activity by immobilization onto copper ferrite nanoparticles for lignin degradation, Int. J. Biol. Macromol. 152 (2020) 1098–1107, https://doi.org/10.1016/j.ijbiomac.2019.10.198.
[62] J. Long, T. Pan, Z. Xie, X. Xu, Z. Jin, Co-immobilization of ß-fructofuranosidase and glucose oxidase improves the stability of Bi-enzymes and the production of lactosucrose, LWT 128 (2020), 109460, https://doi.org/10.1016/j.lwt.2020.109460.
[63] R.M. Bezerra, R.R.C. Monteiro, D.M.A. Neto, F.F.M. da Silva, R.C.M. de Paula, T.L. G. de Lemos, P.B.A. Fechine, M.A. Correa, F. Bohn, L.R.B. Gonçalves, J.C.S. dos Santos, A new heterofunctional support for enzyme immobilization: PEI functionalized Fe3O4 MNPs activated with divinyl sulfone. Application in the immobilization of lipase from Thermomyces lanuginosus, Enzym. Microb. Technol. 138 (2020), 109560, https://doi.org/10.1016/j.enzmictec.2020.109560.
[64] S.M. Hosseini, S.M. Kim, M. Sayed, H. Younesi, N. Bahramifar, J.H. Park, S.H. Pyo, Lipase-immobilized chitosan-crosslinked magnetic nanoparticle as a biocatalyst for ring opening esterification of itaconic anhydride, Biochem. Eng. J. 143 (2019) 141–150, https://doi.org/10.1016/j.bej.2018.12.022.
[65] C.R. Matte, C. Bordinhão, J.K. Poppe, E.V. Benvenutti, T.M.H. Costa, R. C. Rodrigues, P.F. Hertz, M.A.Z. Ayub, Physical-chemical properties of the support immobead 150 before and after the immobilization process of lipase, J. Braz. Chem. Soc. 28 (2017) 1430–1439, https://doi.org/10.21577/0103-5053.20160319.
[66] J. Gracida, T. Arredondo-Ochoa, B.E. García-Almendárez, M. Escamilla-García, K. Shirai, C. Regalado, A. Amaro-Reyes, Improved thermal and reusability properties of xylanase by genipin cross-linking to magnetic chitosan particles, Appl. Biochem. Biotechnol. 188 (2019) 395–409, https://doi.org/10.1007/s12010-018-2928-7.
[67] N.R. Mohamad, N.H.C. Marzuki, N.A. Buang, F. Huyop, R.A. Wahab, An overview of technologies for immobilization of enzymes and surface analysis techniques for immobilized enzymes, Biotechnol. Biotechnol. Equip. 29 (2015) 205–220, https://doi.org/10.1080/13102818.2015.1008192.

[68] R. Li, L. Jiang, L. Ye, J. Lu, H. Yu, Oriented covalent immobilization of esterase BioH on hydrophilic-modified Fe3O4 nanoparticles, Biotechnol. Appl. Biochem. 61 (2014) 603–610, https://doi.org/10.1002/bab.1211.
[69] H.J. Park, A.J. Driscoll, P.A. Johnson, The development and evaluation of ß-glucosidase immobilized magnetic nanoparticles as recoverable biocatalysts, Biochem. Eng. J. 133 (2018) 66–73, https://doi.org/10.1016/j.bej.2018.01.017.
[70] O.S. da Silva, R.L. de Oliveira, J.C. Silva, A. Converti, T.S. Porto, Thermodynamic investigation of an alkaline protease from Aspergillus tamarii URM4634: a comparative approach between crude extract and purified enzyme, Int. J. Biol. Macromol. 109 (2018) 1039–1044, https://doi.org/10.1016/j.ijbiomac.2017.11.081.
[71] H. Eskandarloo, A. Abbaspourrad, Production of galacto-oligosaccharides from whey permeate using ß-galactosidase immobilized on functionalized glass beads, Food Chem. 251 (2018) 115–124, https://doi.org/10.1016/j.foodchem.2018.01.068.
[72] C.J.F. Souza, E.E. Garcia-Rojas, C.S.F. Souza, L.C. Vriesmann, J. Vicente, M.G. de Carvalho, C.L.O. Petkowicz, C.S. Favaro-Trindade, Immobilization of ß-galactosidase by complexation: effect of interaction on the properties of the enzyme, Int. J. Biol. Macromol. 122 (2019) 594–602, https://doi.org/10.1016/j.ijbiomac.2018.11.007.
[73] A. Goel, R. Sinha, S.K. Khare, Immobilization of A. Oryzae ß-galactosidase on silica nanoparticles: development of an effective biosensor for determination of lactose in milk whey, in: P. Shukla (Ed.), Recent Advances in Applied Microbiology, Springer, Singapore, 2017, pp. 3–18, https://doi.org/10.1007/978-981-10-5275-0_1.
[74] X.Y. Chen, M.G. Gänzle, Lactose and lactose-derived oligosaccharides: more than prebiotics? Int. Dairy J. 67 (2017) 61–72, https://doi.org/10.1016/j.idairyj.2016.10.001.
[75] Z.K. Bagewadi, S.I. Mulla, Y. Shouche, H.Z. Ninnekar, Xylanase production from Penicillium citrinum isolate HZN13 using response surface methodology and characterization of immobilized xylanase on glutaraldehyde-activated calcium-alginate beads, 3 Biotech 6 (2016) 1–18, https://doi.org/10.1007/s13205-016-0484-9.
[76] M.L. Verma, C.J. Barrow, J.F. Kennedy, M. Puri, Immobilization of ß-D-galactosidase from Kluyveromyces lactis on functionalized silicon dioxide nanoparticles: characterization and lactose hydrolysis, Int. J. Biol. Macromol. 50 (2012) 432–437, https://doi.org/10.1016/j.ijbiomac.2011.12.029.
[77] C. Huang, Y. Feng, G. Patel, X.Q. Xu, J. Qian, Q. Liu, G.Y. Kai, Production, immobilization and characterization of ß-glucosidase for application in cellulose degradation from a novel Aspergillus versicolor, Int. J. Biol. Macromol. 177 (2021) 437–446, https://doi.org/10.1016/j.ijbiomac.2021.02.154.
[78] M.L. Verma, R. Chaudhary, T. Tsuzuki, C.J. Barrow, M. Puri, Immobilization of ß-glucosidase on a magnetic nanoparticle improves thermostability: application in cellobiose hydrolysis, Bioresour. Technol. 135 (2013) 2–6, https://doi.org/10.1016/j.biortech.2013.01.047.